



Development and application of a novel fluorescent nanosensor based on FeSe quantum dots embedded silica molecularly imprinted polymer for the rapid optosensing of cyfluthrin

Xunjia Li^{a,1}, Hai-Feng Jiao^{b,1}, Xi-Zhi Shi^{a,c,*}, Aili Sun^a, Xiujuan Wang^a, Jiye Chai^a, De-Xiang Li^a, Jiong Chen^a

^a School of Marine Sciences, Ningbo University, 818 Fenghua Road, Ningbo 315211, PR China

^b Ningbo Academy of Oceanology and Fishery, Ningbo 315012, PR China

^c Collaborative Innovation Center for Zhejiang Marine High-efficiency and Healthy Aquaculture, Ningbo 315211, PR China

ARTICLE INFO

Keywords:

FeSe quantum dot
Molecularly imprinted
Cyfluthrin
Determination

ABSTRACT

A novel molecularly imprinted silica layer appended to FeSe quantum dots (MIP-FeSe-QDs) was fabricated and utilized as a recognition element to develop a selective and sensitive fluorescent nanosensor for cyfluthrin (CYF) determination. The MIP-FeSe-QDs were characterized by fluorescence spectrometry, scanning electron microscopy, transmission electron microscopy, and Fourier transform infrared spectroscopy. Excellent selectivity and high sensitivity of MIP-FeSe-QDs to CYF molecules were observed based on the fluorescence quenching of FeSe-QDs. Under optimal conditions, a good linear relationship was found between fluorescence quenching effect and increased CYF concentration within 0.010–0.20 mg/L, with a correlation coefficient of 0.9911. The practicality of the developed sensor method for CYF detection in fish and sediment samples was further validated. Good recoveries ranging from 88.0% to 113.9% with < 6.8% relative standard deviations were obtained. The detection limits of CYF in sediment and fish samples were 1.3 and 1.0 µg/kg, respectively. This study established a novel, rapid fluorescent nanosensor detection method based on MIP-QDs for successfully analyzing CYF in fish and sediment samples.

1. Introduction

Pyrethroid insecticides are important broad-spectrum pesticides widely used to control insects due to their higher efficiency and lower toxicity to mammals than organochlorine and organophosphate insecticides (Li et al., 2017; Saillenfait and Ndiaye, 2015). However, the persistent and massive usage of pyrethroid insecticides has resulted in serious environment and organism-safety problems. Cyfluthrin (CYF) is a type II pyrethroid widely used to control insects in agriculture and has been reportedly detected in coastal sediments collected in California (Lao et al., 2012; Hu et al., 2014). Moreover, long-term exposure to CYF impairs the respiratory system, reproductive function, nervous and immune systems of humans, and non-target organisms, such as aquatic organisms (fish, shrimp, etc.) and bees (Brander et al., 2016; Hughes et al., 2016). Meanwhile, the high stability of CYF in the environment results in the accumulation of their residues in aquatic organisms, which generates adverse effects on aquatic food safety and human health. Therefore, the maximum residue of CYF in food has

been stipulated in many countries, with EU and Japan being the most stringent (Zhang et al., 2016). Developing a rapid, facile, sensitive and reliable quantification method for detection of trace CYF residue is necessary.

Nowadays, high-performance liquid chromatography (HPLC) and gas chromatography (GC) coupled with mass spectrometry are the most important determination methods for target analytes due to their high sensitivity and identification capability (Machado et al., 2017; Mao et al., 2012). However, these methods usually require long operation time, high cost, and tedious sample preparation procedure (Dominguez et al., 2016). Therefore, establishing a simple, rapid, and effective method to detect CYF in environmental and biology samples is urgent.

Quantum dots (QDs) as semiconductor fluorescent nanocrystals are attracting increased attention due to their remarkable optical and electrical properties of stability, broad absorption spectra, sharp symmetric emission band, and high resistance to photo-bleaching, and are thus considered as an excellent signal response candidate for

* Corresponding author at: School of Marine Sciences, Ningbo University, 818 Fenghua Road, Ningbo 315211, PR China.

E-mail address: shixizhi@nbu.edu.cn (X.-Z. Shi).

¹ These authors contributed equally to this work.

designing sensors (Liu et al., 2016; Medintz et al., 2005). Meanwhile, molecular imprinting is an attractive strategy to fabricate tailor-made binding site materials (molecularly imprinted polymers, MIPs) with high selectivity for target molecules similar to the properties of biological antibodies (Panagiotopoulou et al., 2017). Typically, the highly selective MIPs are synthesized through the co-polymerization of functional monomers and cross-linkers in the presence of template molecule. After removal of the template, the complementary imprinting cavities in the shape, size and functional groups to the target molecule onto MIPs were fabricated and allowed specific rebinding to the template. Meanwhile, MIPs are more cost saving, easier to prepare, and possess stronger mechanical and thermal stability compared with biology antibodies (Cumbo et al., 2013). Recently, surface MIPs have been successfully applied as promising recognition elements in sensors, and have exhibited high selectivity for detecting trace contaminants (Shahar et al., 2017; Uzun and Turner, 2016). After surface functionalization of QDs with molecular imprinting, the obtained molecularly imprinted quantum dot materials (MIP-QDs) exhibited a high selectivity to target molecules and excellent fluorescence properties (Chantada-Vázquez et al., 2016). Therefore, the development of the fluorescent nanosensor based on the MIP-QDs has gained considerable attention for the detection of target molecules. Several fluorescent-nanosensor-based MIP-QDs have recently been reported to contain some contaminants, such as organophosphates, phenolic compounds prilocaine, chlorophenol, and clenbuterol (Ensafi et al., 2017; Ye et al., 2011; Huy et al., 2014). However, many QDs based on semiconductor heavy metals (such as CdTe, CdSe) are potential threats to humans and the environment. Therefore, in the present work, novel ecofriendly MIP-QDs based on FeSe-QDs were successfully fabricated and a sensitive fluorescent nanosensor to selectively quench the fluorescence by CYF was initially constructed. The MIP-FeSe-QDs characteristics of morphology, optical stability, and selective fluorescence quenching were investigated. Finally, the application capability of the constructed fluorescent nanosensor based on the MIP-QDs was fully evaluated. The results indicated that the fabricated fluorescent nanosensor-based MIP-FeSe-QDs demonstrated ecofriendly, convenient, rapid, and accurate determination of trace CYF contaminants in sediment and fish samples.

2. Experimental

2.1. Reagents and materials

CYF, bifenthrin (BIF), deltamethrin (DEL), cypermethrin (CYP), and fenvalerate (FEN) were obtained from Shanghai Pesticide Research Institute Co., Ltd (Shanghai, China). Azobisisobutyronitrile (AIBN) was bought from Shanghai Shisihewei Chemical Co., Ltd (Shanghai, China). 3-Aminopropyl-triethoxysilane (APTES), tetraethoxysilane (TEOS), triton X-100, methacrylic acid (MAA), and ethyleneglycol dimethacrylate (EGDMA) were purchased from Sigma-Aldrich (Steinheim, Germany). Ammonia, acetone, chloroform, acetic acid, triethylamine, and cyclohexane were obtained from Sinopharm Group Co., Ltd (Shanghai, China), and all the reagents were of analytical grade.

2.2. Synthesis of FeSe-QDs

The FeSe-QDs were synthesized using the modified method as previously reported (Mao et al., 2014). In a typical experiment, an iron oleate precursor solution was prepared by placing acetylacetone iron, oleic acid, and octadecene in a three-necked flask and evacuated for 1 h at 100 °C. The temperature was increased to 120 °C at 10 °C/min and held until the color of the solution turns from yellow to colorless. Then, it underwent natural cooling to 50 °C. Meanwhile, the appropriate amount of selenium powder and octadecene were quickly added to another three-necked flask and heated at 100 °C for 1 h. The tempera-

ture was then increased to 310 °C at 10 °C/min under nitrogen atmosphere. A 1.0 mL iron oleate precursor solution was injected, and after 0.5 h, a certain amount of chloroform and ethanol were added and centrifuged at 3000 g for 10 min. Finally, the precipitate was redispersed in chloroform to obtain FeSe-QDs.

2.3. Fabrication of MIP-FeSe-QDs

MIP-FeSe-QDs for CYF were synthesized by the modified reverse micro-emulsion method. A total of 40.0 mg of AIBN and 1.8 mL of Triton-X 100 were dissolved in 7.5 mL of cyclohexane in a two-necked flask and stirred for 15 min at 200 rpm. Subsequently, 400 µL of QDs (1 nmol), 50 µL of TEOS, and 100 µL of ammonia were sequentially added and the solution was stirred for 2 h. Meanwhile, the solution mixture containing 4.3 mg of CYF, 21.8 µL of APTES, 3.4 µL of MAA, and 38.1 µL of EGDMA were prepared by stirring for 2 h. Then, the mixture solution was poured into the two-necked flask and stirred for 2 h. Afterwards, the flask was immersed in a 60 °C water bath and allowed to react for 10 h. After polymerization, the MIP-FeSe-QDs were purified by adding 10.0 mL of acetone to the reaction mixture and centrifuged at 8000g for 10 min. After the supernatant was discarded, 6.0 mL of ultrapure water was added and centrifuged at 8000g for 20 min to remove the unreacted crosslinking agent and functional monomer. Finally, the template was removed with ethanol in acetonitrile (8:2, v/v) until the fluorescence value of MIP-FeSe-QDs was not changed as measured by a fluorescence spectrophotometer. Non-imprinted quantum dot materials (NIP-QDs) were simultaneously synthesized in the same process without the addition of template molecules.

2.4. Fluorescent measurements

Fluorescence measurements were performed using a F-4600 fluorescence spectrophotometer (Hitachi, Japan) equipped with a cuvette (1 cm × 1 cm). MIP-FeSe-QDs or NIP-QDs solution was added to the cuvette and mixed with a certain concentration of standard samples for 5 min, and then tested. The parameters for the detection of FL were as follows: the excitation wavelength was 365 nm, the emission wavelength was 450 nm, the slit widths of excitation and emission were both 5 nm, and the photomultiplier voltage was 350 eV. Generally, the determination was performed in triplicate to ensure the measurement accuracy.

2.5. Evaluation of MIP-FeSe-QDs selectivity

Under optimal conditions, the chemical analogs of CYF including BIF, DEL, CYP, and DEL at appropriate concentrations were applied to evaluate the selectivity of the obtained MIP-FeSe-QDs. Furthermore, the selective fluorescence quenching ability of MIP-FeSe-QDs was analyzed by comparing their fluorescence changes after adding different substances. Meanwhile, this system was evaluated by the Stern-Volmer fluorescence quenching equation: $F_0/F = 1 + K_{sv}[Q]$, where F_0 and F in the equation represent the fluorescence values before and after the addition of the quencher, K_{sv} is the quenching constant of the quenching equation, and Q is the concentration of the quencher (Xiao et al., 2016). The values of $\Delta F (F_0 - F)$ were calculated as a response function to evaluate the FL quenching characteristics. The specificity of the MIP-FeSe-QDs was evaluated by the competitive quenching method by fixing CYF concentration and increasing FEN concentration.

2.6. Sample preparation

Marine sediment samples were obtained from Ningbo offshore. The samples were freeze-dried for 24 h and ground. A total of 8 g of sediment samples were weighed and placed in a centrifuge tube; then, 1.0 g of copper powder and 15.0 mL of *n*-hexane in acetone (2: 1, v/v)

were sequentially added. After ultrasonic extraction for 20.0 min, the samples were centrifuged at 9000 rpm for 10.0 min. The samples were extracted repeatedly. The supernatants were combined and underwent rotary evaporation to 2.0 mL. Afterwards, 10.0 mL of cyclohexane was added, passed through a purified column (containing 2 cm in anhydrous sodium sulfate, 3 g of neutral alumina, 2 cm of anhydrous sodium sulfate), evaporated to dryness on a rotary evaporator at 40 °C, and then the residue was re-dissolved in 1.0 mL of cyclohexane for subsequent analysis.

The fish samples were from a local supermarket in Ningbo. Typically, 5.0 g of fish samples were weighed into a 50 mL polypropylene centrifuge tube and homogenized at 8000 rpm for 2 min, then set aside for 2 h. Then, 15.0 mL of acetonitrile and 1.5 g of NaCl were added. After vortexing for 2 min, the samples were centrifuged at 4000 rpm for 5 min. The residues were extracted repeatedly. The supernatants were combined and mixed with 10 mL of acetonitrile:*n*-hexane mixture (1:10, v/v) to remove the fat. After vortexing for 2 min, the acetonitrile was separated by centrifuging at 4000 rpm for 5 min and extracted once again with 10 mL of acetonitrile:*n*-hexane mixture (1:10, v/v). The acetonitrile was then removed in a rotary evaporator at 40 °C. The residue was re-dissolved in 1.0 mL of cyclohexane and filtered through a 0.22 μm nylon filter for subsequent analysis.

3. Results and discussion

3.1. Fabrication and characterization of MIP-FeSe-QDs

A modified reverse microemulsion strategy was used to fabricate the MIP-FeSe-QDs; the scheme for the synthesis process was illustrated in Fig. 1. First, the ecofriendly FeSe quantum dots were synthesized and characterized by fluorescence spectra (Fig. S1). The spatial orientation and type of functional groups on the MIP-FeSe-QDs were previously reported to be the major factors affecting the imprint-

ing site formation and specific template recognition capabilities (Bossi et al., 2001). The higher selectivity at the surface of MIPs silica layer was especially achieved by copolymerizing with the two type of functional monomers (Peng et al., 2010). Therefore, in this study, the molar ratio of MAA functional monomer to template was first optimized to fabricate the high selectivity of MIP-FeSe-QDs. As shown in Fig. S2, the highest fluorescence quenching of MIP-FeSe-QDs was achieved at a ratio of 1:4, and the value was 1399. In contrast, the weaker fluorescence quenching ($\Delta F = 896$) of NIP-QDs to CYF was obtained. The results indicated that the fabricated MIP-FeSe-QDs exhibited the highest selective recognition capability, as well as good fluorescence quenching effect.

The morphology and size distribution of MIP-FeSe-QDs and NIP-QDs were characterized by scanning electron microscopy (SEM) and transmission electron microscopy (TEM), as illustrated in Fig. S3(A, a) and Fig. S3(B, b), respectively. The fabricated MIP-FeSe-QDs possessed uniformly sized spherical morphology and exhibited diameters of approximately 100 nm. The surfaces of the MIP-FeSe-QDs and NIP-QDs were rough, which indicated that the silica layer was coated onto the FeSe-QDs surface. Meanwhile, no distinct difference was found in surface morphology between the MIP-FeSe-QDs and NIP-QDs. Furthermore, to confirm the successful chemical modification onto the QDs, Fourier transform infrared spectroscopy (FT-IR) of MIP-FeSe-QDs and NIP-QDs was performed and compared in Fig. S4. The broad absorption peak at 3421 cm^{-1} represents N–H bending, the peak at 1560 cm^{-1} represents secondary amide N–H bending and C–N stretching, the peak at 2935 cm^{-1} represents C–H stretching, and the peak at 1655 cm^{-1} represents the secondary amide of –CO–NH–, which is attributed to the aminopropyl groups and amide bonding (–CO–NH–) (Zhou et al., 2014). The absorption peaks at 1134 and 1059 cm^{-1} represent Si–O–C and Si–O–Si bond in the polymers, respectively. Other observed bands at approximately 792 and 461 cm^{-1} reveal Si–O vibrations. These peaks suggested the successful

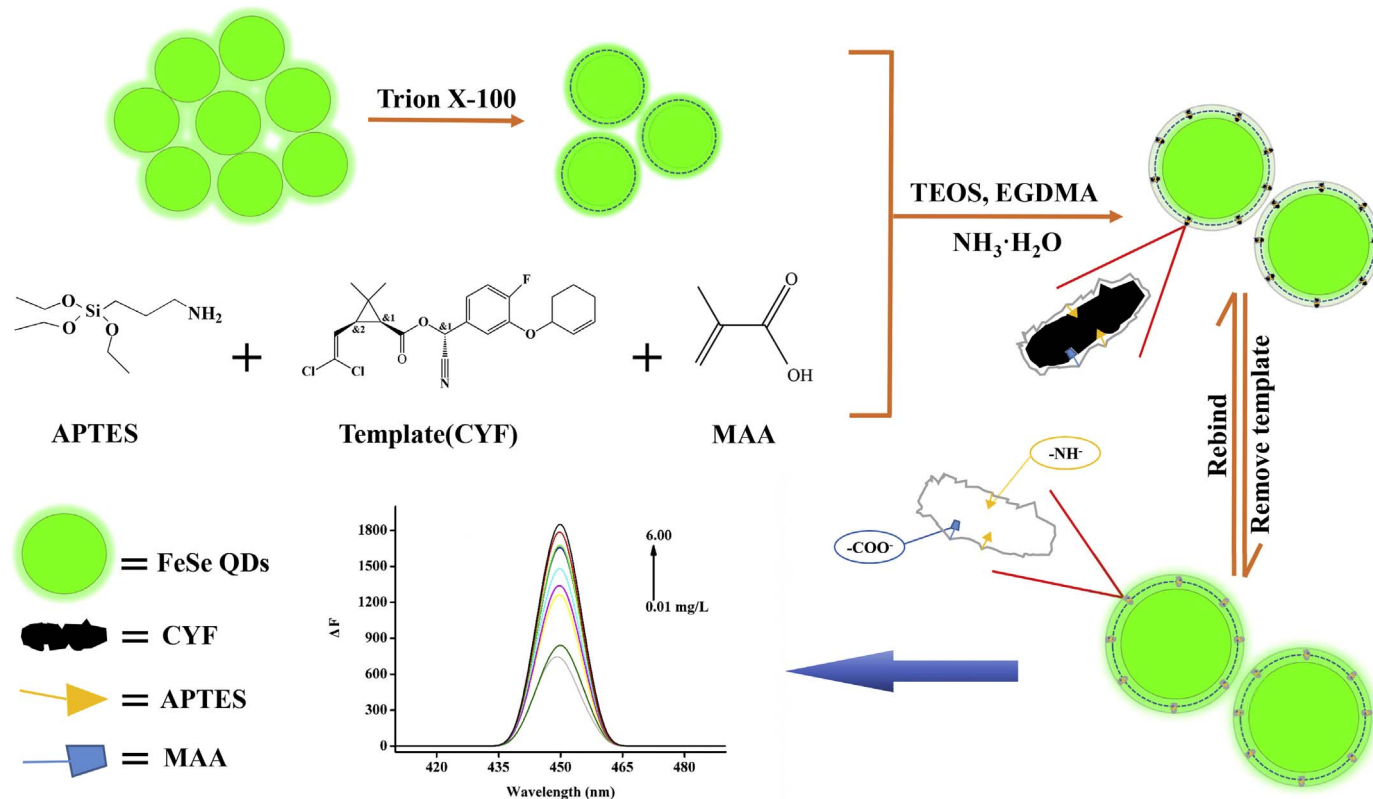


Fig. 1. Schematic of fluorescent nanosensor based on MIP-FeSe-QD.

coating of APTES and MAA onto the FeSe quantum dots through chemical bonding (Xiao et al., 2016). In addition, no obvious difference of major bands in FT-IR spectra between MIP-FeSe-QDs and NIP-QDs was observed, which indicated that their compositions were similar.

Although no distinct difference in the morphology, composition and fluorescence peak wavelength between MIP-FeSe-QDs and NIP-QDs was found, their fluorescence intensities were distinctly different (Fig. S1). Comparing with NIP-QDs, the researchers observed the stronger fluorescence intensity (Fig. S1) and fluorescence quenching of MIP-FeSe-QDs after the addition of the CYF (Fig. S2). The reason may be ascribed to the specific binding of CYF to the $-NH_2/-COOH$ groups of the imprinting cavities that are complementary in size and shape to CYF onto the MIP-FeSe-QDs, which causes significant fluorescence quenching.

3.2. Effect of response time and acetic acid on fluorescence quenching

A certain incubation time is needed for allowing sufficient interactions between CYF and the MIP-FeSe-QDs. Therefore, the experiment proceeded by exposing the MIP-FeSe-QDs to a given concentration of template for ascertaining the response time of the developed sensor. As shown in Fig. S5, after the addition of a template, a fluorescence quenching equilibrium was observed within 5.0 min, and 5.0 min was selected as the response time for subsequent experiments.

The specific fluorescence quenching response of MIP-QDs was affected by the charge of their surface imprinting environment and the chemical structure of the template molecule (Zhang et al., 2011). Therefore, the effects of different ratios of acetic acid to ethanol (0.0% to 5.0%) on fluorescence quenching were investigated. Fig. 2 showed that MIP-FeSe-QDs have a stronger fluorescence quenching (ΔF) than those of NIP-QDs at different concentrations of acetic acid. The largest quenching amount of MIP-FeSe-QDs was obtained in 2.0% acetic acid in ethanol. In contrast, the smallest fluorescence quenching of NIP-QDs corresponds to CYF. With further increased acetic acid concentration in ethanol solution, fluorescence quenching decreased gradually. Furthermore, the effect of triethylamine on fluorescence quenching of MIP-FeSe-QDs were simultaneously investigated. However, we found that the fluorescence intensity and quenching effect of MIP-FeSe-QDs and NIP-QDs were considerably unstable under alkaline condition. These results indicated that the specific interactions between CYF and the imprinting sites onto the MIP-FeSe-QDs mainly occurred by ionic interaction and hydrogen bonding interaction, and the strongly acidic or basic conditions may result in the surface defects of coated layer on MIP-FeSe-QDs and NIP-QDs (Mehrzhad-Samarin et al., 2017). Therefore, 2.0% acetic acid in ethanol was used for further experiments.

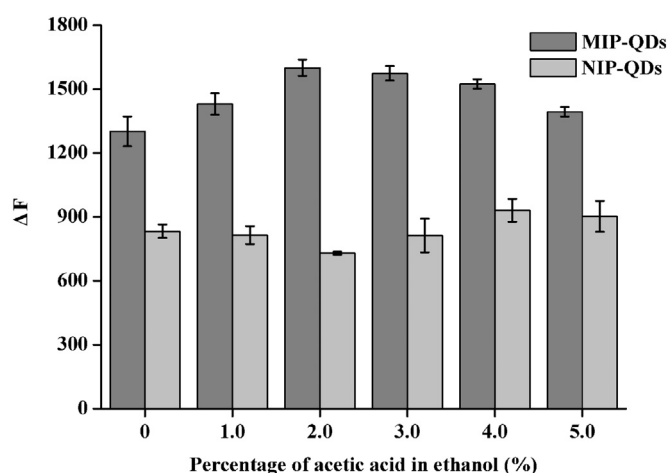


Fig. 2. Influence of acetic acid on the response of MIP-QDs and NIP-QDs. CYF concentration was 0.5 mg/L.

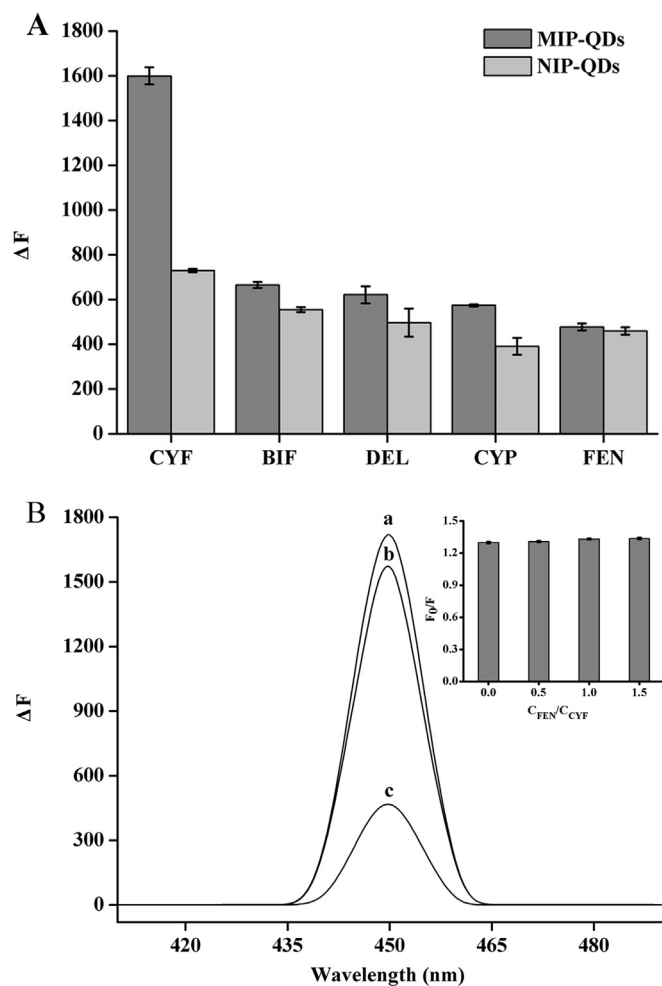


Fig. 3. (A) Selectivity of MIP-QDs and NIP-QDs to CYF, BIF, DEL, CYP, and FEN. (B) Fluorescence quenching response of MIP-QDs after adding (b) CYF, (c) FEN, and (a) their mixture. Inset: influence of different ratios of FEN to CYF on fluorescence quenching response of MIP-QDs. CYF, BIF, DEL, CYP, and FEN concentrations were all 0.5 mg/L. Acetic acid percentage in ethanol was 2%.

3.3. Selectivity of MIP-FeSe-QDs to pyrethroid pesticides

The selectivity of the fabricated MIP-FeSe-QDs was further evaluated by fluorescence quenching response to CYF and its chemical structural analogs, i.e., BIF, DEL, CYP, and FEN. As illustrated in Fig. 3A. The higher fluorescence quenching of CYF to MIP-FeSe-QDs was obtained compared to those of its analogs, which suggested that the specific imprinting cavities to CYF were fabricated on the surface of the MIP-FeSe-QDs. Due to the similar primary compositions with MIP-FeSe-QDs (Fig. S4), the fluorescence of NIP-QDs was also quenched after the addition of CYF, whereas similar low levels of fluorescence quenching effects to CYF and its analogs were found, which indicated disorderly distributed functional base and no specific recognition sites were anchored onto the NIP-QDs surface layers. Further, the selectivity of MIP-FeSe-QDs was confirmed through competitive quenching experiments by fixing CYF concentration and increasing FEN concentration. Fig. 3B illustrated that the fluorescence intensity of MIP-FeSe-QDs was only slightly affected with increased FEN concentration, which indicated that FEN caused weak effect on specific recognition of MIP-FeSe-QDs to CYF. The above results revealed that MIP-FeSe-QDs exhibited a selective recognition and excellent fluorescence quenching response toward CYF, and the molecular size, shape, and functional base of the template complementary to the imprinting cavities are the major dominating factors to the specific fluorescence quenching response.

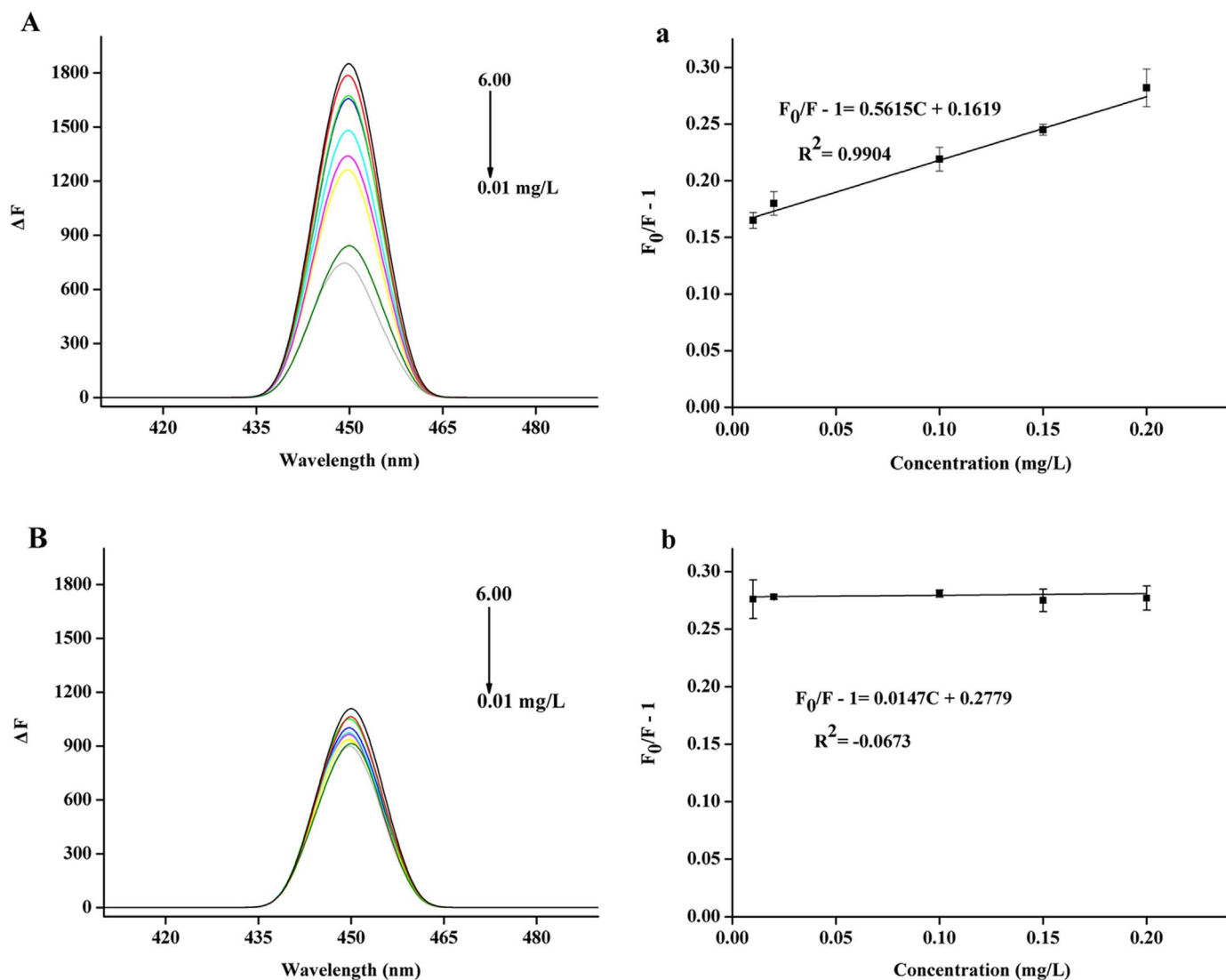


Fig. 4. Fluorescence spectra of (A) MIP-QDs and (B) NIP-QDs with increased CYF concentration. Linear calibration curves for CYF determination by (a) MIP-QDs and (b) NIP-QDs. Acetic acid percentage in ethanol was 2.0%.

3.4. Application to sediments and fish sample analysis

To evaluate the practicality of the developed fluorescent nanosensor for selective and sensitive detection of CYF. The linear relationship between the fluorescence intensity of the MIP-FeSe-QDs and the CYF concentrations was firstly investigated. Fig. 4 showed that the fluorescence intensity of MIP-FeSe-QDs was quenched gradually with increased CYF concentration. Comparing with those of NIP-QDs, the researchers found that the fluorescence quenching values of MIP-FeSe-QDs at different concentrations all increased, which indicated a blotting site with a specific site for CYF on the surface of MIP-QDs. The fluorescence quenching response of the MIP-QDs followed the Stern–Volmer equation. The good linear relationship in the concentration range of 0.010 mg/L to 0.20 mg/L with a correlation coefficient of 0.9911 for CYF, and the relative standard deviation (RSD) values of each concentration below 10.0%, were obtained.

Furthermore, the sensor was applied to the selective and sensitive detection of CYF in marine sediment and fish samples. No CYF was found by GC-MS in the real samples. the accuracy and precision were simultaneously evaluated by the recovery and RSD, respectively. The appropriate quantities of CYF were spiked into the real samples. The results were summarized in Table 1. The achieved recoveries of sediment samples were in the range of 107.5–113.9% with the RSDs

Table 1

Analysis of cyfluthrin in spiked sediment and fish ($n=3$).

Sample	Spike (mg/kg)	Recovery (%)	RSD (%)
Sediments	0.01	113.9	3.0
	0.1	107.5	3.9
	0.2	113.6	0.9
Fish	0.02	89.7	6.1
	0.1	90.7	6.8
	0.2	88.0	4.2

< 3.9%. The recoveries of fish samples were in the range of 88.0–90.7% with the RSD < 6.8%, which indicated that the developed fluorescent nanosensor techniques based on MIP-FeSe-QDs had good applicability in the detection of CYF in sediments and fish samples. These results indicated that the accuracy and precision of the developed fluorescent nanosensor were acceptable for the determination of CYF in real samples. The LOD, which was calculated as the CYF concentration of the fluorescence quenching corresponding to three times the value of the standard deviation of the blank sample, was 1.3 and 1.0 $\mu\text{g}/\text{kg}$ in sediment and fish samples, respectively. Furthermore, as summarized in Table S1, the fabricated fluorescent nanosensor based on the MIP-FeSe-QDs for CYF detection was comparable or better than those

reported in the reference of linearity range and LOD as listed in the literature. Therefore, the developed fluorescent nanosensor in this work exhibited excellent practicability for the sensitive determination of CYF in real sediment and fish samples.

4. Conclusions

In present study, the ecofriendly FeSe-QDs were successfully developed. Furthermore, the MIP-FeSe-QDs that specifically fluoresce quenching response to CYF were synthesized by modified reverse micro-emulsion and characterized by fluorescence spectrometry, SEM, TEM and FT-IR. The possible imprinting and selective fluorescence quenching properties of the MIP-FeSe-QDs were further evaluated by fluorescence quenching response to CYF and its chemical structural analogs. After the specific recognition of MIP-FeSe-QDs to CYF by ionic interaction, shape selectivity and hydrogen bonding interaction, the charge transfer from the FeSe-QDs to CYF could be blocked and resulted in the fluorescence quenching of the MIP-FeSe-QDs. Furthermore, under optimal conditions, the fluorescent nanosensor based on MIP-FeSe-QDs for the selective determination of CYF was constructed and exhibited excellent linearity, selectivity and sensitivity. Finally, the proposed fluorescent nanosensor provided a rapid, simple and sensitive detection system for CYF in fish and sediment samples and exhibited good accuracy, precision and the low detection limits of 1.0 and 1.3 $\mu\text{g}/\text{kg}$ in fish and sediment samples, respectively. Thus, we provided a novel system based on MIP-FeSe-QDs for rapid detection of CYF in fish and sediments samples. The potential advantages of this detection strategy, such as ecofriendly, simple preparation and excellent sensitivity, will attract more and more attentions for wide application in the near future.

Acknowledgments

This work was supported by the National Natural Science Foundation of China (No. 31372572), the Zhejiang Provincial Natural Science Foundation of China (LR16C190001, LY15C190002), the Public Science and Technology Research Funds Projects of Ocean (No. 201405035), the Technology Innovation Team of Ningbo City (2015C110018), the project by Ningbo Science and Technology Bureau (No. 2014C10063), the project of Zhejiang Provincial Food and Drug Administration (2015002), supported by the Open Fund of Zhejiang Provincial Top Key Discipline of Aquaculture in Ningbo University (xkzsc1515), and the K.C. Wong Magna Fund in Ningbo University.

Appendix A. Supporting information

Supplementary data associated with this article can be found in the online version at doi:10.1016/j.bios.2017.07.071.

References

- Bossi, A., Piletsky, S.A., Piletska, E.V., Righetti, P.G., Turner, A.P., 2001. *Anal. Chem.* 73, 5281–5286.
- Brander, S.M., Gabler, M.K., Fowler, N.L., Connon, R.E., Schlenk, D., 2016. *Environ. Sci. Technol.* 50, 8977–8992.
- Chantada-Vázquez, M.P., Sánchez-González, J., Peña-Vázquez, E., Tabernero, M.J., Bermejo, A.M., Bermejo-Barrera, P., Moreda-Piñeiro, A., 2016. *Biosens. Bioelectron.* 75, 213–221.
- Cumbo, A., Lorber, B., Corvini, P.F.-X., Meier, W., Shahgaldian, P., 2013. *Nat. Commun.* 4, 1503.
- Domínguez, I., González, R.R., Liébanas, F.J.A., Vidal, J.L.M., Frenich, A.G., 2016. *Trac-Trend Anal. Chem.* 12, 1–12.
- Ensafi, A.A., Kazemifard, N., Rezaei, B., 2017. *Sens. Actuators B-Chem.* 242, 835–841.
- Hu, G.P., Zhao, Y., Song, F.Q., Liu, B., 2014. *Res. Microbiol.* 165, 110–118.
- Hughes, M.F., Ross, D.G., Starr, J.M., Scollon, E.J., Wolansky, M.J., Crofton, K.M., Devito, M.J., 2016. *Toxicology* 19, 359–360.
- Huy, B.T., Seo, M.-H., Zhang, X., Lee, Y.-I., 2014. *Biosens. Bioelectron.* 57, 310–316.
- Lao, W., Tiefenthaler, L., Greenstein, D.J., Maruya, K.A., Bay, S.M., Ritter, K., Schiff, K., 2012. *Environ. Toxicol. Chem.* 31, 1649–1656.
- Li, H., Cheng, F., Wei, Y., Lydy, M.J., You, J., 2017. *J. Hazard Mater.* 324, 258–271.
- Liu, Y., Liu, L., He, Y., He, Q., Ma, H., 2016. *Biosens. Bioelectron.* 77, 886–893.
- Machado, I., Gêrez, N., Pistón, M., Heinzen, H., Cesio, M.V., 2017. *Food Chem.* 227, 227–236.
- Mao, X., Wan, Y., Yan, A., Shen, M., Wei, Y., 2012. *Talanta* 97, 131–141.
- Mao, X., Kim, J.G., Han, J., Jung, H.S., Lee, S.G., Kotov, N.A., Lee, J., 2014. *J. Am. Chem. Soc.* 136, 7189–7192.
- Medintz, I.L., Uyeda, H.T., Goldman, E.R., Mattoussi, H., 2005. *Nat. Mater.* 4, 435–446.
- Mehrzad-Samarin, M., Faridbod, F., Dezfuli, A.S., Ganjali, M.R., 2017. *Biosens. Bioelectron.* 92, 618–623.
- Panagiotopoulou, M., Kunath, S., Medina-Rangel, P.X., Haupt, K., Bui, B.T.S., 2017. *Biosens. Bioelectron.* 88, 85–93.
- Peng, Y., Xie, Y., Luo, J., Nie, L., Chen, Y., Chen, L., Du, S., Zhang, Z., 2010. *Anal. Chim. Acta* 674, 190–200.
- Saillenfait, A.M., Ndiaye, D., 2015. *Int. J. Hyg. Environ. Health* 218, 281–292.
- Shahar, T., Siron, T., Mandler, D., 2017. *Nano Res.* 10, 1056–1063.
- Uzun, L., Turner, A.P., 2016. *Biosens. Bioelectron.* 76, 131–144.
- Xiao, T.-T., Shi, X.-Z., Jiao, H.-F., Sun, A.-L., Ding, H., Zhang, R.-R., Pan, D.-D., Li, D.-X., Chen, J., 2016. *Biosens. Bioelectron.* 75, 34–40.
- Ye, T., Lu, S.Y., Hu, Q.Q., Jiang, X., Wei, G.F., Wang, J.J., Lu, J.Q., 2011. *Chin. Chem. Lett.* 22, 1253–1256.
- Zhang, W., He, X.-W., Chen, Y., Li, W.-Y., Zhang, Y.-K., 2011. *Biosens. Bioelectron.* 26, 2553–2558.
- Zhang, X., Yang, S., Sun, L., Luo, A., 2016. *J. Mater. Sci.* 51, 6075–6085.
- Zhou, Y., Qu, Z.-B., Zeng, Y., Zhou, T., Shi, G., 2014. *Biosens. Bioelectron.* 52, 317–323.